

# Comparison of ultrasonic suture welding and traditional knot tying in a rabbit rotator cuff repair model

Shane J. Nho, MD,<sup>a</sup> Brian J. Cole, MD, MBA,<sup>a</sup> Augustus D. Mazzocca, MD,<sup>b</sup> James M. Williams, PhD,<sup>c</sup> Anthony A. Romeo, MD,<sup>a</sup> Charles A. Bush-Joseph, MD,<sup>a</sup> Bernard R. Bach, Jr, MD,<sup>a</sup> and Nadim J. Hallab, PhD,<sup>d</sup> Chicago, IL, and Farmington, CT

*The purpose of this study is to evaluate ultrasonic suture welding of monofilament suture in an animal model of rotator cuff repair with biomechanical and histologic analyses. We randomly assigned 46 shoulders in 23 rabbits to 1 of 3 treatment groups: sham-operated (n = 15), knotted (n = 15), and welded (n = 16). Supraspinatus defects were surgically created and acutely repaired with suture anchors loaded with either No. 2-0 Ethibond for knotted group or No. 2-0 nylon for welded shoulders. Eighteen weeks postoperatively, all animals were killed, and the shoulders underwent either biomechanical testing or histologic analysis. The maximum stress of the sham-operated group (20.6 N/mm<sup>2</sup>) was significantly greater than that of both the knotted (10.2 N/mm<sup>2</sup>) and welded (8.3 N/mm<sup>2</sup>) groups (P < .05), but no differences were observed between the knotted and welded groups. Although some histologic changes were noted, none was considered to be significant to distinguish either group. (J Shoulder Elbow Surg 2006;15:630-638.)*

Over the past 10 years, the treatment of rotator cuff pathology has evolved toward an all-arthroscopic approach. Arthroscopic rotator cuff repair is believed to be at least as effective as open repair, with the

added advantages of reduced surgical morbidity, reduced postoperative stiffness, and potentially, a more rapid return to baseline shoulder function once rotator cuff healing has occurred.<sup>35</sup> In addition, arthroscopically performed repairs avoid detachment or manipulation of the deltoid muscle, leading to decreased postoperative pain, and virtually eliminate the risk for deltoid detachment.<sup>35</sup>

Despite the benefits of an arthroscopic approach, many orthopaedic surgeons prefer open or miniopen repairs because of the technical skills required to perform an all-arthroscopic approach.<sup>23-25,30</sup> Surgeons must choose from different suture material, knot-tying techniques, and uniquely designed instruments. Specifically, suture passing, anchor placement, and suture tying are particularly challenging for even the most experienced arthroscopists. Mastering a relatively steep learning curve is required to become facile at these techniques. Even in experienced hands, obtaining consistent and secure arthroscopic knots is difficult compared with openly tied knots, and arthroscopic knots are, therefore, prone to failure.<sup>23</sup>

The arthroscopic knot may be the final obstacle preventing many orthopaedic surgeons from advancing to all-arthroscopic repair. Arthroscopic knots are required to secure tendon-to-tendon sutures and tendon-to-bone sutures via suture anchors. Poorly positioned, loose, or unstable knots will inevitably lead to failure. *In vitro* studies have demonstrated that suture slippage, rather than suture breakage, is often the failure point with arthroscopic rotator cuff repair. Even minimal amounts of suture elongation or knot slippage of only 3 mm can lead to clinical evidence of repair failure.\*

Ultrasonic suture welding is an arthroscopic instrument that uses 70 kHz of ultrasonic energy to melt a nonabsorbable monofilament suture together without damaging the underlying soft tissue. A recent *in vitro* study comparing the mechanical properties of ultrasonic suture welding and traditional knot tying demonstrated that welded loops required significantly greater loads to reach 3 mm of elongation.<sup>33</sup> The number of cycles to failure was similar in both groups, but the knotted loop demonstrated increased variabil-

From the <sup>a</sup>Section of Sports Medicine, Rush Medical College, Rush University Medical Center, Chicago, <sup>b</sup>Department of Orthopaedic Surgery, University of Connecticut School of Medicine, Farmington, OSC-MSp2, <sup>c</sup>Department of Anatomy and Cell Biology, <sup>d</sup>Department of Orthopedic Surgery, Rush Medical College, Rush University Medical Center, Chicago, IL.

Supported by the Rush Sport Medicine Fund, Rush University Medical Center, Chicago, IL, and the AOA Student Research Fellowship, Menlo Park, CA.

Reprint requests: Brian J. Cole, MD, MBA, Associate Professor, Section of Sports Medicine, Department of Orthopedic Surgery, Rush Medical College, Rush University Medical Center, 1725 W Harrison St, Suite 1063, Chicago, IL 60612 E-mail: bcole@rushortho.com.

Copyright © 2006 by Journal of Shoulder and Elbow Surgery Board of Trustees.

1058-2746/2006/\$32.00

doi:10.1016/j.jse.2005.09.006

\*References 4, 15-18, 23-25, 34, 39, 40, 42, 43, 48.

ity compared with the welded loop. The elongation to suture rupture was significantly greater in the knotted loops, but both groups had greater knot strength than that for No. 2 nonabsorbable braided sutures.<sup>33</sup> Ultrasonic suture welding is an innovative method that directly addresses the difficulty of arthroscopic knot tying and may be used in any procedure that requires arthroscopically placed knots.

Ultrasonic suture welding of nylon suture offers an alternative to hand knot tying that may allow the orthopaedic surgeon to place consistent and reliable suture loops in an all-arthroscopic manner. Whereas *in vitro* studies have demonstrated a more consistent loop and superior strength of welded loops compared with traditional knotted loops at 3 mm of elongation,<sup>33</sup> *in vivo* examination of welded sutures in rotator cuff repair has not been investigated. This is the first study to evaluate ultrasonic suture welding in an *in vivo* rabbit rotator cuff repair model. The aim of this study is to compare the biomechanical strength of the ultrasonic suture loops with that of traditionally tied knots and to describe the gross and histologic features. We hypothesize that, using an *in vivo* animal model of rotator cuff repair, ultrasonic suture loops can repair a detached supraspinatus tendon with a biomechanical strength similar to that of traditionally tied knots.

## MATERIALS AND METHODS

### Experimental design

The Institutional Animal Care and Use Committee of Rush University Medical Center (Chicago, IL) approved all methods before beginning the study. We obtained 23 male New Zealand white rabbits (4-6 lb) and coded them with numbered ear tags. We randomly assigned 46 shoulders to 1 of 3 treatment groups: sham-operated ( $n = 15$  shoulders), knotted ( $n = 15$ ), or welded ( $n = 16$ ). On day 0, all animals were anesthetized and underwent surgery. The supraspinatus tendon was exposed and left intact in all sham-operated shoulders. In the 2 repair groups, the supraspinatus tendon was incised at its insertion into the greater tuberosity of the humeral head, and the artificially created defect was repaired acutely with either traditionally tied knots (knotted group) or ultrasonic suture welded loops (welded group). Eighteen weeks after surgery, all animals were killed. Ten shoulders from each group (ie, sham-operated, knotted, and welded) were removed for biomechanical testing, and five shoulders were assigned to undergo histologic analysis with the exception of the welded group, which had an additional shoulder for histologic analysis. Animals were inspected daily by the staff of the Comparative Research Center of Rush University Medical Center (Chicago, IL).

### Surgical procedure

Each rabbit was anesthetized with an intramuscular injection of a ketamine and xylazine cocktail (75-100 mg/kg and 10 mg/kg, respectively). The upper extremities



**Figure 1** Ultrasonic suture welding with No. 2-0 nylon suture.

were shaved and aseptically prepared for the surgical procedure. An incision through the skin and subcutaneous tissue was made just proximal to the acromial process and extended to the proximal humerus. The deep fascia was incised along the cranial margin of the acromial portion of the deltoid muscle, and the muscle was retracted caudally. The supraspinatus tendon was easily visualized, and the extremity was internally rotated to also identify the infraspinatus tendon. For sham-operated shoulders, the supraspinatus tendon was isolated but no tear was created. For experimental shoulders, the supraspinatus tendon was identified and a 5-mm full-thickness anteroposterior incision was created 1 mm from the insertion into the humeral head to create a complete tear of the supraspinatus tendon. A single 2.0-mm titanium anchor (Orthopaedic Biosystems Ltd, Smith & Nephew, Andover, MA) was inserted at a 45° angle.<sup>5</sup> For knotted shoulders, a simple suture configuration was used, such that only one limb of the suture penetrated the supraspinatus tendon 5 mm into the substance of the tendon. A standard arthroscopic knot was used (5 half-hitches with the first 2 placed over the same post in the same direction and the subsequent 3 as alternating posts and alternating throws)<sup>6,7</sup> with a No. 2-0 Ethibond suture (Ethicon Inc, Somerville, NJ), and the knot was placed directly over the rotator cuff tendon with an arthroscopic knot pusher (Arthrex, Inc, Naples, FL). For welded shoulders, the supraspinatus tendon was repaired with an ultrasonic suture welding device (Axya Medical Inc, Beverly, MA) via a single No. 2-0 nylon suture placed through the suture anchor. The tensioning arm must cross over the nontensioning arm within the AxyaWeld handpiece J-tips (Axya Medical Inc). The slide button on the handpiece can be moved from the open position to the advance position. The nontensioning arm should be longer than the tensioning arm so that the surgeon can pull the suture tighter on the soft tissue. The tensioning arm is grasped as the welding sleeve is advanced to the repair site, and the suture and soft tissue are held taught underneath the J-tip. The welding sleeve must face the soft tissue at an angle between 20° and 70° to the surface. Once the desired suture loop tension is obtained, the slide button can be advanced to the weld position and pressed to weld the suture together (Figure 1). The slide button is released back to the open position, and the distal

tip of the welding sleeve can be gently pressed into the soft tissue to release from the welded suture. Arthroscopic suture scissors (Arthrex, Inc) were used to cut the tails of the suture at about 1 mm from the welded portion of the loop. The repair site was inspected to ensure that the supraspinatus tendon was reapproximated to the greater tuberosity without evidence of a gap. For all shoulders, the previously incised deltoid was approximated anatomically. Anteroposterior and lateral plain radiographs were obtained from selected rabbits to ensure proper placement of suture anchors. Once the animals recovered from surgery, they were placed in isolated cages and permitted to ambulate without restrictions. All animals received buprenorphine (0.3 mg/mL) analgesia on the evening of surgery, postoperative day 1, and postoperative day 2.

### Macroscopic analysis

At week 18, all rabbits were sedated with an intramuscular injection of ketamine (50 mg/kg) and killed with an intracardiac injection of 5 mL potassium chloride. The shoulder region was dissected immediately after death, and the operated area was examined for healing, suture encapsulation, suture elongation, suture slippage, suture breakage, loose bodies, and inflammatory reaction. The supraspinatus insertion into the humerus with or without a suture loop was identified and left intact.

### Biomechanical analysis

The specimens (humerus and supraspinatus tendon) for biomechanical analysis were wrapped in saline solution-soaked gauze, placed in 2 plastic bags, and frozen at  $-20^{\circ}\text{C}$ . On the day of biomechanical testing, specimens were thawed at room temperature and kept moistened with phosphate-buffered saline solution throughout testing. The thickness and width of each supraspinatus tendon were measured with digital calipers (Precision Graphic Instruments, Inc, Spokane, WA), and the same investigator was blinded to the experimental groups and performed all measurements. A dumbbell-shaped specimen was created by use of a scalpel at the supraspinatus insertion site with a minimum width of 5 mm and a gauge length of 10 mm,<sup>8</sup> and the shape at the midpoint of the defect appeared to have a rectangular cross-sectional area. The cross-sectional area was calculated as the product of the measured thickness and width. The humerus was potted in a 1.5-in-diameter and 4-in-long cylindrical pipe with bone cement (Isocryl; Lang Dental, Deerfield, IL), leaving only the humeral head and supraspinatus tendon exposed. The free end of the supraspinatus tendon was placed in the cryoclamp (Blue Bay Research, Clearwater, FL), and the chutes of the cryoclamp were loaded with dry ice. Specimen strain was measured via the crosshead displacement of the Instron mechanical testing machine (Instron model 8871; Instron, Canton, MA). Tissue strain was measured by laser extensometer (MTS, Minneapolis, MN) monitoring of photomarkers placed on the tendon specimens. The photomarkers for the laser extensometer were placed at 3 mm and 8 mm from the tendon insertion. The laser extensometer was positioned at 381 mm from the sample and calibrated before testing. The potted tendons were placed in a clamp at a  $20^{\circ}$  angle from the horizontal axis, and the cryoclamp was fastened to

the load cell on a material testing system so that the supraspinatus tendon was pulled at the physiologic angle of  $110^{\circ}$ .<sup>8</sup> A tensile load was applied to each specimen at a constant displacement rate of 15 mm/min, and the test was allowed to continue until a final displacement change of 40 mm was achieved. The load, crosshead displacement, and tissue strain were recorded by use of Instron computer software. The specimen strain and specimen modulus were determined by the load cell and crosshead displacement, but the tissue strain and tissue modulus were calculated from the laser extensometer. These results were subsequently exported and analyzed on a spreadsheet (Microsoft Excel 2000; Microsoft Corp, Richmond, WA) in order to determine the maximum load, stress, tissue strain, specimen strain, tissue modulus, and specimen modulus.

### Microscopic analysis

After gross examination, the humerus was detached from the scapula, with the supraspinatus tendon and muscle being kept intact, and then fixed in 10% neutral buffered formalin. Samples were decalcified in aqueous formic acid/sodium citrate (22%/10%), after which they were processed for paraffin embedding. After decalcification, the suture loops and suture anchors for the knotting and welding-treated supraspinatus tendons were carefully removed. Sections for histologic analysis (8  $\mu\text{m}$ ) were obtained and placed on glass slides coated with Vectabond (Vector Laboratories, Burlingame, CA) from the entire width of the attachment of the supraspinatus tendon to the humerus. Alternating sections were stained with safranin O, fast green,<sup>36</sup> to demonstrate proteoglycan, hematoxylin-eosin, or picosirius red. Sections through the central region of the tendon were studied in detail.

Collagen orientation of the repaired tendon was examined by use of the picosirius red staining method.<sup>10,19,27,28</sup> Slides containing sections were placed in xylene at  $37^{\circ}\text{C}$  for 12 hours to remove the strongly birefringent paraffin completely, hydrated in an ethanol series of decreasing concentration (between 100% and 50%), and then placed in water. Hydration was used immediately after the removal of paraffin and before staining for collagen with picosirius red F3B (Polysciences, Inc, Warrington, PA). Before staining with a picosirius red solution, dewaxed and hydrated sections were treated at  $37^{\circ}\text{C}$  for 18 hours in 2.0 mg bovine testicular hyaluronidase in 1.0 mL of 0.1-mol/L phosphate buffer at pH 6.0 to remove chondroitin sulfate molecules, which might mask the cationic binding sites of the collagen for the polyamine sirius red molecules.<sup>29</sup> Sections were then stained for 30 minutes in 0.1% sirius red F3B (Polysciences, Inc, Warrington, PA) dissolved in saturated picric acid. Sections were dehydrated in absolute ethanol for 9 minutes (3 changes for 3 minutes each), cleared in a 1:1 mixture of absolute ethanol-xylene for 3 minutes, and dehydrated in xylene for 9 minutes (3 changes for 3 minutes each) before cover slips were mounted. Stained sections were analyzed with a Nikon polarization microscope (Fryer Company, Huntley, IL) equipped with a lambda/4 compensator plate and interference filter ( $\lambda = 589\text{ nm}$ ). The relative sign of induced birefringence was determined by turning the analyzer in two opposite directions. The optical properties of the extracellular matrix—that is, the presence or absence of birefringence, indicating orientation of the collagen fibers<sup>10,19,27,28</sup>—were observed.

Normal light microscopic observations were made in the same visual fields where polarization microscopic analyses were carried out. For normal light microscopy, the polarizer and interference filter were removed from the microscope.

The histologic sections were examined by use of a custom scoring system based on that used by Carpenter et al<sup>8</sup> but also accounted for (1) transition zone architecture in hematoxylin-eosin-stained sections, (2) collagen fiber orientation in picosirius red-stained sections, (3) proteoglycan staining in safranin O-stained sections, and (4) bursa thickness in hematoxylin-eosin-stained sections. In addition, a number of other histologic features were noted, including articular cartilage, inflammation, foreign-body reaction, vascularity, and cellularity.

### Statistical analysis

All measurements were entered into a statistical spreadsheet (SPSS for Windows, version 10.0; SPSS, Inc, Chicago, IL), and descriptive statistics were calculated for the cross-sectional area of the dumbbell-shaped region of the supraspinatus tendon, maximum load, stress, strain, and modulus for all shoulders. Paired *t* tests for right and left shoulders demonstrated no statistical difference ( $P > .05$ ) for surface area, maximum load to failure, stress, and strain. One-way analysis of variance was performed between the different treatment groups, and post hoc analysis with Bonferroni-corrected *t* tests was performed for tests considered to be significant.  $P < .05$  was considered to be statistically significant.

## RESULTS

### Surgical procedure

All animals survived without complications until they were killed 18 weeks after the operation. In two knotted shoulders, the initial suture anchor pulled out while the Ethibond suture was being tightened but the subsequent suture anchor with an Ethibond knot was securely fixed in the humeral head. The first 3 attempts to screw in the suture anchor failed in another knotted shoulder, but the fourth anchor appeared to be fixed firmly with axial loading. In one of the welded shoulders, the loop ruptured immediately after application of the ultrasonic suture welding device. This shoulder was not included in the final analysis; thus, there were 15 shoulders in the welded group, instead of 16 shoulders.

### Macroscopic analysis

Upon macroscopic analysis, the sham-operated shoulders had minimal scarring of the deltoid muscle. The supraspinatus tendon was intact without any gross abnormalities. The repaired shoulders revealed an extensive degree of scar tissue from the supraspinatus insertion to the undersurface of the deltoid. Although quantitative measurements were not made, the welded loops were less bulky and lower in profile compared with the knotted loops. In the knotted should-

**Table 1** Supraspinatus tendon measurements of experimental groups

Group	Animal weight (kg)	Cross-sectional area (mm <sup>2</sup> )
Sham (n = 10)	8.99 ± 0.88	10.47 ± 2.06
Knotted (n = 10)	8.61 ± 0.79	17.45 ± 5.05
Welded (n = 10)	8.89 ± 0.77	20.93 ± 10.27*
Analysis of variance (P value)	.573	.009

Data are presented as mean ± SD.

\*Denotes statistical significance from sham-operated group at  $P < .01$ .

ers, the Ethibond knot was encapsulated in a scar tissue mass. One of the knotted shoulders appeared to have a healed, mildly displaced humeral head fracture, which was most likely a result of the insertion of the suture anchor. Loose, small suture fragments were observed in 2 welded shoulders, but the welded loop in each case was intact. Another welded shoulder contained a calcified mass just superior to the sutured tendon. There were no specimens with gap formation between the tendon and humeral head. There was no evidence of suture elongation, suture slippage, or suture breakage for any repaired supraspinatus tendons.

### Biomechanical analysis

The cross-sectional area was significantly greater in the knotted (17.5 mm<sup>2</sup>,  $P = .001$ ) and welded (21.0 mm<sup>2</sup>,  $P = .008$ ) groups than in the sham-operated group (10.5 mm<sup>2</sup>) (Table I). Although the maximum load to failure of the knotted (161.9 N) and welded (161.6 N) groups was less than that of the sham-operated group (206.4 N), only the stress of the experimental groups (10.2 N/mm<sup>2</sup> and 8.3 N/mm<sup>2</sup>, respectively) was statistically inferior to the control group (20.6 N/mm<sup>2</sup>) ( $P = .002$  and  $P = .0001$ , respectively). The repaired supraspinatus tendons of both experimental groups were approximately 80% of the tensile strength of the intact supraspinatus tendons (78.42% for knotted group and 78.27% for welded group). There were no detectable statistical differences between the knotted and welded groups. All specimens failed at the tendon-to-bone junction, and the suture anchor was intact in all 30 specimens. In addition, there were no apparent differences observed between any group for tissue strain, specimen strain, tissue modulus, and specimen modulus (Table II).

### Microscopic analysis

In all specimens, there was good integration of tendon-to-bone healing without any evidence of the surgically created defect. Apart from the thickening of the subdeltoid bursa, there were no histologic signs of

**Table II** Biomechanical characteristics of experimental groups

Group	Maximum load (N)	Stress (N/mm <sup>2</sup> )	Tissue strain at failure	Specimen strain at failure	Tissue modulus (N/mm <sup>2</sup> )	Specimen modulus (N/mm <sup>2</sup> )
Sham (n = 10)	206.41 ± 47.45	20.63 ± 7.46	0.29 ± 0.10	0.21 ± 0.16	50.74 ± 21.58	332.90 ± 276.50
Knotted (n = 10)	161.86 ± 63.28	10.24 ± 5.10*	0.30 ± 0.12	0.15 ± 0.15	36.36 ± 12.70	338.19 ± 214.12
Welded (n = 10)	161.55 ± 85.36	8.32 ± 3.84†	0.33 ± 0.15	0.18 ± 0.17	32.45 ± 17.60	303.32 ± 249.67
Analysis of variance (P value)	.279	.0001	.631	.803	.762	.072

Data are presented as mean ± SD.

\*Denotes statistical significance from sham-operated group at  $P < .001$ .

†Denotes statistical significance from sham-operated group at  $P < .0001$ .

acute inflammatory changes in any specimen. In addition, there were no abnormalities in any specimen in terms of the articular cartilage of the humeral head, vascularity, and cellularity.

In all sham-treated specimens, the transition zone architecture was regular, with clearly demarcated zones of tendon, unmineralized fibrocartilage, mineralized fibrocartilage, and bone (Figure 2, A). Dense regular collagen fibers could be seen in all samples (Figure 2, B). Also, an intervening subdeltoid bursa was apparent between the supraspinatus tendon and the overlying deltoid muscle fibers in all specimens (Figure 2, C). In 2 of 5 specimens, a random arrangement of collagen fibers could be seen in the articular side of the tendon in the picosirius red-stained section, and increased proteoglycan staining was also observed in the same area in the safranin O-stained sections (Figure 2, D). The herring-bone appearance was consistent with a fibrocartilage differentiation within the substance of these two tendons that was observed on the articular side of the supraspinatus tendon adjacent to the tendon-to-bone insertion.

Four of five knotted specimens demonstrated regular transition zone architecture with tendon fibers interdigitating with trabecular bone. Dense, longitudinally oriented collagen fibers were visible in all samples. In 4 of 5 knotted specimens, mild subdeltoid bursa thickening with loosely arranged connective tissue was noted (Figure 3). One specimen was found to have irregular transition zone architecture with poor collagen fiber arrangement of the tendon zone. Ethibond suture fragments surrounded by moderately irregular collagen orientation in the immediate area were found in 1 supraspinatus tendon. Proteoglycan staining was absent in all knotted specimens.

In 4 of 5 welded specimens, regular transition zone architecture was observed. Dense longitudinal collagen fibers were observed in 2 of 5 welded specimens. Moderate or marked subdeltoid bursal thickening was also observed in all welded samples (Figure 4, A). Three of five welded specimens had irregular collagen fiber orientation with correspond-

ing increased proteoglycan staining consistent with a herring-bone pattern. In 1 specimen, a widened fibrocartilage zone of the articular side was seen, and evidence of early bone formation of the bursal side could be demonstrated (Figure 4, B).

## DISCUSSION

As anticipated, the results of the biomechanical tests indicate that the stress to failure was significantly reduced in the knotted and welded groups when compared with the sham-operated controls. The maximum load to failure of the knotted and welded groups was less than that in the sham-operated group, but the difference was not statistically significant. In contrast, the mean cross-sectional area for the knotted and welded groups was significantly larger than that in the sham-operated group; thus, the stress (maximum load divided by cross-sectional area) of the sham-operated group was statistically greater than that in the knotted and welded groups. Even though the mean cross-sectional area was greater in the knotted and welded groups, the repaired supraspinatus tendons proved to be weaker than the intact supraspinatus tendons, implying that the integrity of the repaired tendon differs from that of native tendon, which has been observed in the repaired tendons of other animal models.<sup>8,41</sup> There was no statistically significant difference between the knotted and welded groups in terms of stress, strain, or modulus. The maximum load to failure for the knotted and welded groups was approximately 80% of that for the sham-operated tendons. Miyahara et al<sup>26</sup> evaluated tendon-to-bone healing in a dog model and demonstrated that load to failure was roughly 62.5% at 6 weeks and 82.5% at 24 weeks. Gerber et al<sup>14</sup> concluded that strength of reattached infraspinatus tendons in sheep was 30% at 6 weeks and was 81% at 6 months compared with that in native tendons. Blevins et al<sup>3</sup> also demonstrated restoration of 80% of normal strength in cynomolgus monkeys 1 year after surgical repair of the rotator cuff with transosseous

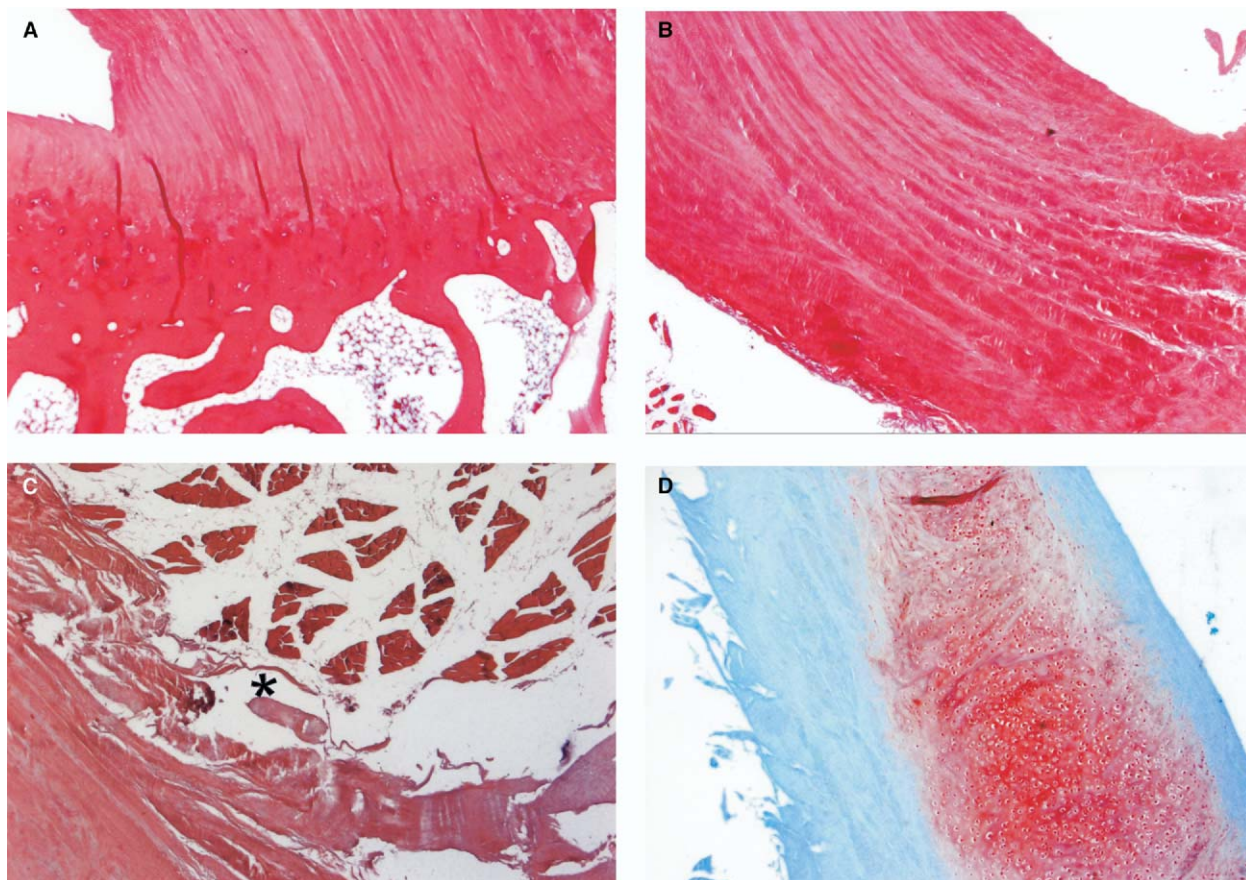


**Figure 2** Histologic sections (original magnification  $\times 20$ ) of sham operated group. **A**, Tendon-to-bone interface with tendon, unmineralized fibrocartilage, mineralized fibrocartilage, and bone zones with hematoxylin-eosin. **B**, Collagen fiber orientation in regular longitudinal arrangement stained with hematoxylin-eosin. **C**, Sham-operated group with thin subdeltoid bursa (asterisk) between supraspinatus tendon and deltoid muscle stained with hematoxylin-eosin. **D**, Herring-bone appearance in selected sham-operated specimens with safranin O staining. The area of increased safranin O staining was observed on the articular side of the supraspinatus tendon adjacent to the tendon-to-bone insertion.

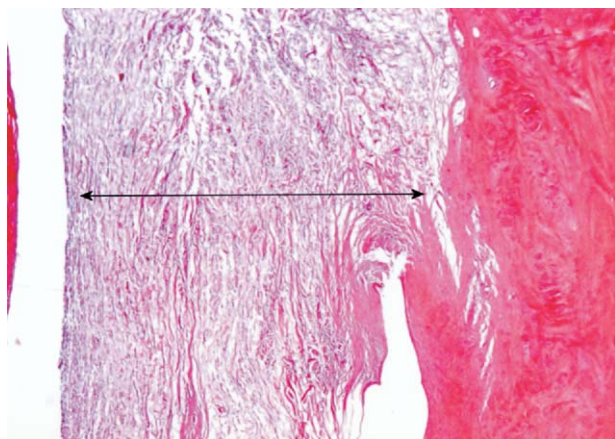


**Figure 3** Histologic section (original magnification  $\times 20$ ) of knotted group, with moderately thickened subdeltoid bursa. The arrow demonstrates the extent of subdeltoid bursal thickening.

tunnels. There was no evidence of impaired healing with the suture anchor, and longer-term studies are required to determine whether biomechanical strength continues to improve in the knotted and welded groups.

The primary objective of this study was to evaluate the biomechanical and histologic characteristics of supraspinatus tendons repaired with ultrasonic suture welded loops and traditionally tied knots at a time point reflective of a healed supraspinatus tendon. Prior studies, characterizing the healing process of repaired rabbit rotator cuff tendons, have shown ongoing remodeling to occur up to 12 weeks<sup>13</sup>; thus, one relatively late time point at 18 weeks was thought to provide an adequate comparison of the biomechanical strength of healed supraspinatus tendons. Although earlier time points may have strengthened the study, we chose to focus on the clinical efficacy of

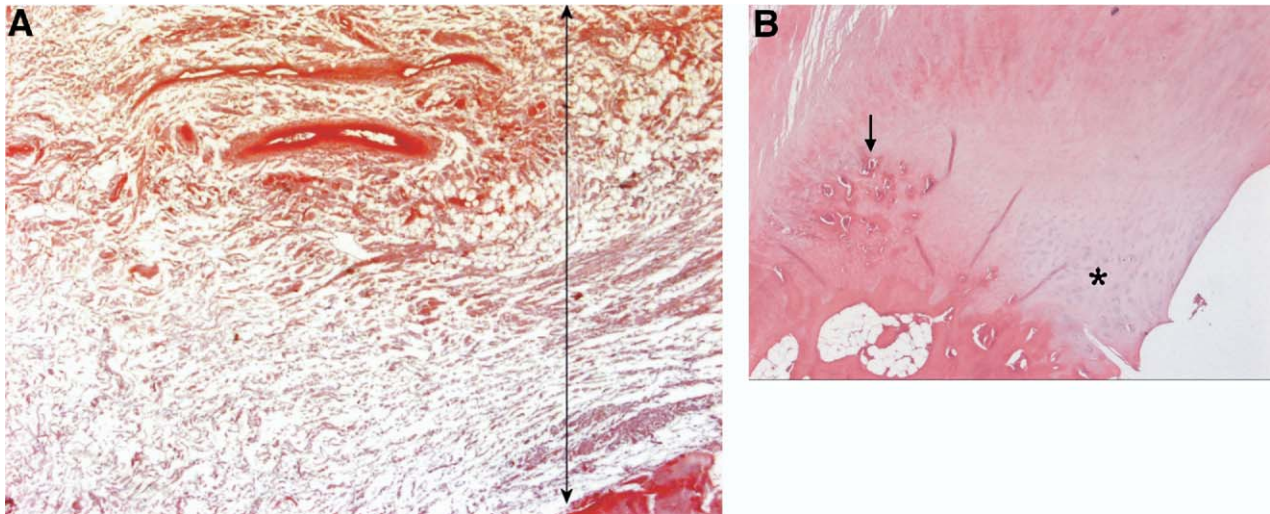


**Figure 4** Histologic sections (original magnification  $\times 20$ ) of welded group. **A**, Marked thickening of subdeltoid bursa. The *arrow* demonstrates the extent of subdeltoid bursal thickening. **B**, weld specimen with area of widened fibrocartilage on articular side (*asterisk*) and early bone formation of bursal side (*arrow*).

two different suture fixation techniques on tendon-to-bone healing. Previous studies of ultrasonic suture welding in New Zealand white rabbits did not show evidence of thermal injury to underlying tissue at time 0 and at 1 week by gross and histologic analysis.<sup>9,33</sup> The purpose of the earlier time points would have been to determine evidence of thermal injury, which, if present, might impair the healing response. Additional time points may provide more information, but we submit that, based on prior studies, there is no reason to suggest that thermal injury occurs in surrounding tissue. If so, we expect that the earlier time points would reveal similar histologic healing for both the hand-tied knot specimens and the ultrasonically welded suture loop specimens. Future *in vivo* studies with multiple time points and a larger sample size are required to demonstrate definitively the effect of ultrasonic energy to surrounding soft tissues.

The biomechanical method has a number of limitations that may have affected the precision of the results. Digital calipers were used to measure the width and thickness of each specimen, which may vary depending on the amount of pressure applied. We acknowledge that optical or indentation probe techniques are preferred, but the same investigator was blinded to experimental groups and measured all specimens. The specimen preparation involved the creation of a dumbbell-shaped defect at the tendon-to-bone interface. The tendon-to-bone junction proved to be able to withstand greater loads than was initially anticipated. Once cryoclamps were implemented, numerous pilot studies demonstrated that the junction of the humeral head and cylindrical pipe was the most common point of failure. Uthoff et al<sup>47</sup> also experienced difficulty with the biomechanical setup,

and they used a compression bolt in the medullary canal to augment the fixation of the humerus. Despite these interventions, they experienced failure at points other than the tendon-to-bone insertion, including the bone, clamp, and tendon midsubstance. In addition, Gerber et al<sup>14</sup> encountered tearing of the sheep infraspinatus tendon at the clamp. In our study, the dumbbell-shaped defect was created in the supraspinatus tendon, beginning at the tendon-to-bone junction and extending proximally into the tendon substance. With the dumbbell-shaped defect, the failure point at the tendon-to-bone junction was consistently produced and meaningful comparison between the experimental groups was possible. The specimens were kept moist with phosphate-buffered saline solution; however, a phosphate-buffered saline solution bath provides a more accurate environment to control for hydration, pH, and temperature. The testing time only required roughly 60 to 90 seconds, and there was no gross evidence of tendon tissue compromise, and biomechanical properties appeared to be unaltered. Future studies will be performed in a phosphate-buffered bath to control for the aforementioned factors.

The transition zone architecture was relatively preserved, except in 1 case in each of the experimental groups. The most notable feature of the knotted group was the presence of a mildly thickened subdeltoid bursa. The welded group also possessed thickening of the subdeltoid bursa but to a greater degree. There appeared to be a qualitative difference between the knotted and welded groups, which is surprising given the lower profile and absence of the knot of the welded sutures to irritate the bursa. An inflammatory response after surgical detachment and repair of the

supraspinatus tendon is expected, but the etiology and significance of the differing responses are unclear. No obvious thermal injury to the tendon occurred with the ultrasonic suture welder at the time of surgery, and no evidence of thermal necrosis was evident upon histologic analysis at 18 weeks after surgery. The different suture materials could be another possible explanation for the differing bursa responses. There may be clinical implications if there is a significant difference between the knotted and welded groups, but additional studies with a larger sample size are necessary. Prior studies of tendon-to-bone healing have noted that the injured tendon is unable to regain completely normal structure and strength<sup>3</sup>; however, these tissues do retain a considerable capacity to heal.<sup>46</sup> Uthoff et al<sup>44,46</sup> have suggested that the initial healing response may largely be derived from the bursal tissue and advise against bursectomy with rotator cuff tendon repair. The bursal thickening observed in the experimental groups, but not the sham-treated group, may suggest an ongoing healing response after repair of the supraspinatus tendon and contribute to greater cross-sectional area of the repaired tendons.

Because of the lack of an appropriate animal model, Soslowky et al<sup>38</sup> conducted a study to determine the most suitable animal for studying the potential mechanisms of rotator cuff disease. Of all 33 animals considered, only the rat satisfied all 34 items on the checklist and has an acromion that was positioned immediately over a prominent supraspinatus tendon. The authors acknowledge the superiority of the rat or primates for studies to further delineate the etiology or pathophysiology of rotator cuff tendinopathy, particularly involving the subacromion. The rabbit rotator cuff model has been used by several other groups to characterize tendon-to-bone healing,<sup>2,21</sup> because the transition zone architecture is preserved across species. Unfortunately, pilot studies with several rat shoulders performed in our laboratory resulted in humeral head fracture with the insertion of 1.3-mm titanium screw-in suture anchor (Mitek Worldwide, Norwood, MA), which is even smaller than the 2.0-mm suture anchor used in our study. The rabbit was selected because of size considerations and the primary goal of characterizing the healing of the tendon-to-bone interface between two different suture fixation techniques. The lack of an acromion in the rabbit shoulder makes it difficult to comment on the significance of the subdeltoid bursal thickening observed in the experimentally repaired groups. These findings may have clinical implications after rotator cuff repair possibly leading to impingement; therefore, longer-term studies with a rat or primate model may further delineate the significance of the bursal thickening. In addition, prospective clinical studies with radiographic imaging may be able

to correlate postsurgical subacromial bursal thickening with patient symptoms.

The majority of studies evaluating rotator cuff repair investigate either tendon-to-bone healing via transosseous tunnels<sup>12,20,22,31,41,45</sup> or *ex vivo* biomechanical analyses of suture anchors.<sup>1,11,15,32,37</sup> Our study was designed to characterize an innovative arthroscopic technology in an *in vivo* model so that we might be able to determine whether the suture anchor, suture material, or suture fixation methods interfere with tendon-to-bone healing. We submit that fixation devices should withstand a minimum amount of load, but it is the healing of the tendon-to-bone interface and ongoing remodeling process that will determine the effectiveness of the repair. On the basis of our results, we believe that both techniques—arthroscopic knot tying with Ethibond and ultrasonic suture welding with nylon—are functionally efficacious and may be used according to surgeon preference. Longer-term studies with a larger sample size are required to determine the significance of the histologic discrepancy observed between the 3 treatment groups.<sup>49</sup>

## REFERENCES

1. Apreleva M, Ozbaydar M, Fitzgibbons PG, Warner JJ. Rotator cuff tears: the effect of the reconstruction method on three-dimensional repair site area. *Arthroscopy* 2002;18:519-26.
2. Björkenheim JM, Paavolainen P, Ahovuo J, Slati P. Resistance of a defect of the supraspinatus tendon to intraarticular hydrodynamic pressure: an experimental study on rabbits. *J Orthop Res* 1990;8:175-9.
3. Blevins FT, Djurasovic M, Flatow EL, Vogel KG. Biology of the rotator cuff tendon. *Orthop Clin North Am* 1997;28:1-16.
4. Brouwers JE, Oosting H, de Haas D, Kloppe PJ. Dynamic loading of surgical knots. *Surg Gynecol Obstet* 1991;173:443-8.
5. Burkhart SS. The deadman theory of suture anchors: observations along a south Texas fence line. *Arthroscopy* 1995;11:119-23.
6. Burkhart SS. A stepwise approach to arthroscopic rotator cuff repair based on biomechanical principles. *Arthroscopy* 2000;16:82-90.
7. Burkhart SS, Wirth MA, Simonich M, Salem D, Lanctot D, Athanasios K. Knot security in simple sliding knots and its relationship to rotator cuff repair: how secure must the knot be? *Arthroscopy* 2000;16:202-7.
8. Carpenter JE, Thomopoulos S, Flanagan CL, DeBano CM, Soslowky IJ. Rotator cuff defect healing: a biomechanical and histologic analysis in an animal model. *J Shoulder Elbow Surg* 1998;7:599-605.
9. Connolly R, Egan T. A histologic comparison of welded suture loops to knotted suture loops in an animal model. Boston, MA: New England Medical Center, Surgical Research Laboratory. p. 1-3.
10. Constantine VS, Mowry RW. Selective staining of human dermal collagen. II. The use of picosirius red F3BA with polarization microscopy. *J Invest Dermatol* 1968;50:419-23.
11. Cummins CA, Strickland S, Appleyard RC, Szomor ZL, Marshall J, Murrell GA. Rotator cuff repair with bioabsorbable screws: an *in vivo* and *ex vivo* investigation. *Arthroscopy* 2003;19:239-48.
12. DeJardin IM, Arnoczky SP, Ewers BJ, Haut RC, Clarke RB. Tissue-engineered rotator cuff tendon using porcine small intestine



- submucosa. Histologic and mechanical evaluation in dogs. *Am J Sports Med* 2001;29:175-84.
13. Fuhrmann R, Mollenhaur J, Kircher S, Wiederanders B, Venbrocks R. Alteration in collagen pattern impairs tissue properties after osseous reinsertion of the supraspinatus tendon. In: Transactions of the Orthopaedic Research Society; Dallas, Tex; Feb 10-13, 2002.
  14. Gerber C, Schneeberger AG, Perren SM, Nyffeler RW. Experimental rotator cuff repair. A preliminary study. *J Bone Joint Surg Am* 1999;81:1281-90.
  15. Gerber C, Schneeberger AG, Beck M, Schlegel U. Mechanical strength of repairs of the rotator cuff. *J Bone Joint Surg Br* 1994;76:371-80.
  16. Gunderson PE. The half-hitch knot: a rational alternative to the square knot. *Am J Surg* 1987;154:538-40.
  17. Herrmann JB. Tensile strength and knot security of surgical suture materials. *Am Surg* 1971;37:209-17.
  18. Holmlund DE. Knot properties of surgical suture materials. A model study. *Acta Chir Scand* 1974;140:355-62.
  19. Junqueira LC, Bignolas G, Brentani RR. Picrosirius staining plus polarization microscopy, a specific method for collagen detection in tissue sections. *Histochem J* 1979;11:447-55.
  20. Kimura A, Aoki M, Fukushima S, Ishii S, Yamakoshi K. Reconstruction of a defect of the rotator cuff with polytetrafluoroethylene felt graft. Recovery of tensile strength and histocompatibility in an animal model. *J Bone Joint Surg Br* 2003;85:282-7.
  21. Kumagai J, Sarkar K, Uthoff HK. The collagen types in the attachment zone of rotator cuff tendons in the elderly: an immunohistochemical study. *J Rheumatol* 1994;21:2096-100.
  22. Liu SH, Panossian V, al-Shaikh R, Tomin E, Shepherd E, Finerman GA, Lane JM. Morphology and matrix composition during early tendon to bone healing. *Clin Orthop Relat Res* 1997;253-60.
  23. Loutzenheiser TD, Harryman DT II, Yung SW, France MP, Sidles JA. Optimizing arthroscopic knots. *Arthroscopy* 1995;11:199-206.
  24. Loutzenheiser TD, Harryman DT II, Ziegler DW, Yung SW. Optimizing arthroscopic knots using braided or monofilament suture. *Arthroscopy* 1998;14:57-65.
  25. Mishra DK, Cannon WD Jr, Lucas DJ, Belzer JP. Elongation of arthroscopically tied knots. *Am J Sports Med* 1997;25:113-7.
  26. Miyahara H, et al. A morphologic and biomechanical study on the healing of the repaired rotator cuff insertion in dogs: a preliminary report. In: Post M, Morrey BF, Hawkins RJ, editors. *Surgery of the shoulder*. St Louis: Mosby; 1990. p. 224-7.
  27. Modis L. Experimental reconstruction of the oriented glycosaminoglycan structure of the extracellular matrix. In: *Organizations of extracellular matrix: a polarization microscopic approach*. Boca Raton (FL): CRC Press; 1991. p. 157-76.
  28. Modis L. Factors involved in formation and maintenance of oriented microstructure of matrix constituents. In: *Organizations of extracellular matrix: a polarization microscopic approach*. Boca Raton (FL): CRC Press; 1991. p. 177-206.
  29. Modis L. Methodological appendix. In: *Organizations of extracellular matrix: a polarization microscopic approach*. Boca Raton (FL): CRC Press; 1991. p. 265-82.
  30. Nottage WM, Lieurance RK. Arthroscopic knot typing techniques. *Arthroscopy* 1999;15:515-21.
  31. Oguma H, Murakami G, Takahashi-Iwanaga H, Aoki M, Ishii S. Early anchoring collagen-fibers at the bone-tendon interface are conducted by woven bone formation: light microscope and scanning electron microscope observation using a canine model. *J Orthop Res* 2001;19:873-80.
  32. Reed SC, Glossop N, Ogilvie-Harris DJ. Full-thickness rotator cuff tears. A biomechanical comparison of suture versus bone anchor techniques. *Am J Sports Med* 1996;24:46-8.
  33. Richmond JC. A comparison of ultrasonic suture welding and traditional knot tying. *Am J Sports Med* 2001;29:297-9.
  34. Rodeheaver GT, Thacker JG, Edlich RF. Mechanical performance of polyglycolic acid and polyglactin 910 synthetic absorbable sutures. *Surg Gynecol Obstet* 1981;153:835-41.
  35. Romeo AA, Cohen BS, Cole BJ. Arthroscopic repair of full thickness rotator cuff tears: surgical technique and instrumentation. *Orthop Special Ed* 2001;7:25-30.
  36. Rosenberg L. Chemical basis for the histological use of safranin O in the study of articular cartilage. *J Bone Joint Surg Am* 1971;53:69-82.
  37. Rossouw DJ, McElroy BJ, Amis AA, Emery RJ. A biomechanical evaluation of suture anchors in repair of the rotator cuff. *J Bone Joint Surg Br* 1997;79:458-61.
  38. Soslowky IJ, Carpenter JE, DeBano CM, Banerji I, Moalli MR. Development and use of an animal model for investigations on rotator cuff disease. *J Shoulder Elbow Surg* 1996;5:383-92.
  39. Taylor FW. Surgical knots. *Ann Surg* 1938;107:458-68.
  40. Tera H, Aberg C. Tensile strengths of twelve types of knot employed in surgery, using different suture materials. *Acta Chir Scand* 1976;142:1-7.
  41. Thomopoulos S, Hattersley G, Rosen V, Mertens M, Galatz L, Williams GR, et al. The localized expression of extracellular matrix components in healing tendon insertion sites: an in situ hybridization study. *J Orthop Res* 2002;20:454-63.
  42. Trimbos JB, Booster M, Peters AA. Mechanical knot performance of a new generation polydioxanone suture (PDS-2). *Acta Obstet Gynecol Scand* 1991;70:157-9.
  43. Trimbos JB, Van Rijssel EJ, Klopper PJ. Performance of sliding knots in monofilament and multifilament suture material. *Obstet Gynecol* 1986;68:425-30.
  44. Uthoff HK, Kumagai J, Sarkar K. Morphologic evidence of healing in torn human rotator cuffs. *J Bone Joint Surg Br* 1992;74:293-4.
  45. Uthoff HK, Sano H, Trudel G, Ishii H. Early reactions after reimplantation of the tendon of supraspinatus into bone. A study in rabbits. *J Bone Joint Surg Br* 2000;82:1072-6.
  46. Uthoff HK, Sarkar K, Kumagai J. In vitro behaviour of ruptured human rotator cuff. *J Bone Joint Surg Br* 1992;74:22.
  47. Uthoff HK, Seki M, Backman DS, Trudel G, Himori K, Sano H. Tensile strength of the supraspinatus after reimplantation into a bony trough: an experimental study in rabbits. *J Shoulder Elbow Surg* 2002;11:504-9.
  48. van Rijssel EJ, Trimbos JB, Booster MH. Mechanical performance of square knots and sliding knots in surgery: comparative study. *Am J Obstet Gynecol* 1990;162:93-7.
  49. Vogel KG, Keller EJ, Lenhoff RJ, Campbell K, Koob TJ. Proteoglycan synthesis by fibroblast cultures initiated from regions of adult bovine tendon subjected to different mechanical forces. *Eur J Cell Biol* 1986;41:102-12.